

Thermodynamic and Transport Properties of $\text{H}_2/\text{H}_2\text{O}/\text{NaB}(\text{OH})_4$ Mixtures Using the Delft Force Field ($\text{DFF}/\text{B}(\text{OH})_4^-$)

Parsa Habibi,^{†,‡} Julien R. T. Postma,[¶] Johan T. Padding,[¶] Poulumi Dey,[‡] Thijs J.
H. Vlugt,[†] and Othonas A. Moulτος^{*,†}

[†]*Engineering Thermodynamics, Process & Energy Department, Faculty of Mechanical
Engineering, Delft University of Technology, Leeghwaterstraat 39, 2628 CB Delft, The
Netherlands*

[‡]*Department of Materials Science and Engineering, Faculty of Mechanical Engineering,
Delft University of Technology, Mekelweg 2, 2628 CD Delft, The Netherlands*

[¶]*Complex Fluid Processing, Process & Energy Department, Faculty of Mechanical
Engineering, Delft University of Technology, Leeghwaterstraat 39, 2628 CB Delft, The
Netherlands*

E-mail: o.moulτος@tudelft.nl

Force field parameters (Tables S1 - S3); Additional info on MD and CFCMC simulations (Tables S4 - S5); Raw data of MD simulations for self-diffusivities (Tables S6); Raw data of CFCMC simulations (Table S7); Densities of aqueous NaB(OH)_4 solutions using different B(OH)_4^- force fields (Figure S1); Densities of aqueous NaB(OH)_4 solutions using the TIP4P/ μ force field of water (Figure S2); Viscosities of pure water (Figure S3); Finite-size effects of computed electrical conductivities (Figure S4).

Table S1: Force field parameters for TIP4P/2005¹ and TIP4P/ μ developed in the Supporting Information of Ref.² σ and ϵ are the Lennard-Jones parameters, q is the atomic partial charge, and l is the bond length. σ and l are in units of Å, ϵ is in units of kJ/mol, and q is in units of the elementary charge e . In the TIP4P/2005¹ force field, the charge on O is on a massless site M.

	TIP4P/2005 ¹	TIP4P/ μ ²
$\text{H} - \widehat{\text{O}} - \text{H} (\text{°})$	104.52	104.52
$l_{\text{O-H}}$	0.9572	0.9572
$l_{\text{O-M}}$	0.1546	0.1546
σ_{OO}	3.1589	3.1589
σ_{HH}	0	0
ϵ_{OO}	0.774908	0.663989
ϵ_{HH}	0	0
q_{O}	0	0
q_{M}	-1.1128	-1.06272
q_{H}	0.5564	0.53136

Table S2: Force field parameters for three-site Marx³ hydrogen. σ and ϵ are the Lennard-Jones parameters, q is the atomic partial charge, dummy site L is the geometric center of mass, and l is the bond length. σ and l are in units of Å, ϵ is in units of kJ/mol, and q is in units of the elementary charge e .

σ_{LL}	2.958
ϵ_{LL}	0.305141
q_{H}	0.468
q_{L}	-0.936
$l_{\text{H-H}}$	0.74

Table S3: Parameters for the Madrid-Transport^{4,5} and Madrid-2019⁶ force fields of Na^+ . σ and ϵ are the Lennard-Jones parameters and q is the atomic partial charge. O refers to the O-atom of water. σ is units of Å, ϵ is in units of kJ/mol, and q is in units of the elementary charge e .

	Madrid-Transport	Madrid-2019
$\sigma_{\text{Na}^+\text{Na}^+}$	2.21737	2.21737
$\sigma_{\text{Na}^+\text{O}}$	2.38725	2.60838
$\epsilon_{\text{Na}^+\text{Na}^+}$	1.472356	1.472356
$\epsilon_{\text{Na}^+\text{O}}$	0.793388	0.793388
q_{Na^+}	0.75	0.85

Table S4: The numbers of water molecules or ions (N) used in the MD simulations to compute densities, viscosities, and self-diffusivities of H_2 , Na^+ , and $\text{B}(\text{OH})_4^-$ in aqueous $\text{NaB}(\text{OH})_4$ solutions. m is in units of mol $\text{NaB}(\text{OH})_4/\text{kg}$ water. To obtain self-diffusivities of H_2 , 2 H_2 molecules are used at molalities of 1, 3, and 5 mol $\text{NaB}(\text{OH})_4/\text{kg}$ water. The simulations at 0.5 and 4 mol $\text{NaB}(\text{OH})_4/\text{kg}$ water are only carried out for computing ionic conductivities. For each molality, the same numbers of molecules and ions are used for all temperatures. The average box volume ($\langle V \rangle$) in units of \AA^3 is shown for each molality at 298 K and 1 bar.

m	$N_{\text{H}_2\text{O}}$	N_{Na^+}	$N_{\text{B}(\text{OH})_4^-}$	$\langle V \rangle$
0.5	1000	9	9	30458
1.00	1000	18	18	30924
3.00	1000	54	54	32828
4.00	1000	72	72	33805
5.00	1000	90	90	34798

Table S5: The numbers of water molecules or ions (N) used in Continuous Fractional Component Monte Carlo (CFCMC)⁷⁻⁹ simulations to compute activities of water and solubilities of H_2 in aqueous $\text{NaB}(\text{OH})_4$ solutions. m is in units of mol $\text{NaB}(\text{OH})_4/\text{kg}$ water. For each molality, the same numbers of molecules and ions are used for all temperatures. In every simulation, a single fractional molecule of H_2 used. The average box volume ($\langle V \rangle$) in units of \AA^3 is shown for each molality at 298 K and 1 bar.

m	$N_{\text{H}_2\text{O}}$	N_{Na^+}	$N_{\text{B}(\text{OH})_4^-}$	$\langle V \rangle$
0	300	0	0	9041
0.93	300	5	5	9293
2.96	300	16	16	9874
5.00	300	27	27	10481

Table S6: Results of Molecular Dynamics (MD) simulations for finite-size corrected^{10,11} self-diffusivities of H₂O ($D_{\text{H}_2\text{O}}$), Na⁺ (D_{Na}), B(OH)₄⁻ ($D_{\text{B(OH)}_4}$), and H₂ (D_{H_2}) in aqueous NaB(OH)₄ solutions at 1 bar using the DFF/B(OH)₄⁻ model developed in this work (see Table 1 of the main text), combined with the Na⁺ model of Madrid-2019,⁶ the TIP4P/2005¹ H₂O force field, and the Marx³ H₂ force field. T is in units of K, m is in units of mol NaB(OH)₄/kg water, C is in units of mol NaB(OH)₄/L solution, ρ is in units of kg/m³, and η is in units of mPa·s. $D_{\text{H}_2\text{O}}$, D_{Na} , $D_{\text{B(OH)}_4}$, and D_{H_2} are in units of 10⁻⁹ m²/s. σ_x is the standard deviation of quantity x .

T	m	C	ρ	σ_ρ	η	σ_η	$D_{\text{H}_2\text{O}}$	$\sigma_{D_{\text{H}_2\text{O}}}$	D_{Na}	$\sigma_{D_{\text{Na}}}$	$D_{\text{B(OH)}_4}$	$\sigma_{D_{\text{B(OH)}_4}}$	D_{H_2}	$\sigma_{D_{\text{H}_2}}$
298	1.00	0.96	1063.7	0.2	1.11	0.10	1.89	0.13	1.02	0.06	0.78	0.07	3.73	0.18
298	3.00	2.73	1186.9	0.2	2.50	0.22	1.05	0.07	0.54	0.04	0.40	0.03	2.01	0.13
298	5.00	4.29	1294.3	0.3	5.45	0.52	0.55	0.02	0.28	0.01	0.20	0.01	1.19	0.21
323	1.00	0.95	1050.8	0.1	0.76	0.06	3.07	0.16	1.69	0.07	1.28	0.12	5.79	0.26
323	3.00	2.68	1168.0	0.1	1.41	0.05	1.85	0.06	1.01	0.03	0.74	0.04	3.54	0.17
323	5.00	4.20	1269.9	0.3	2.67	0.08	1.1	0.02	0.60	0.01	0.42	0.01	2.41	0.21
333	1.00	0.95	1044.6	0.1	0.61	0.02	3.75	0.13	2.13	0.06	1.59	0.06	6.94	0.51
333	3.00	2.66	1160.1	0.1	1.16	0.06	2.26	0.06	1.26	0.04	0.93	0.04	4.61	0.17
333	5.00	4.17	1260.3	0.2	2.34	0.26	1.335	0.08	0.73	0.04	0.52	0.04	2.96	0.18
343	1.00	0.94	1038.1	0.1	0.52	0.00	4.475	0.09	2.53	0.05	1.94	0.06	7.71	0.99
343	3.00	2.65	1151.9	0.1	1.01	0.06	2.669	0.15	1.49	0.06	1.08	0.06	5.57	0.12
343	5.00	4.14	1250.7	0.2	1.77	0.10	1.706	0.06	0.95	0.02	0.68	0.03	3.43	0.32
353	1.00	0.93	1031.1	0.1	0.48	0.02	5.035	0.14	2.75	0.10	2.17	0.11	9.02	0.55
353	3.00	2.63	1143.7	0.2	0.94	0.12	3.084	0.16	1.76	0.12	1.25	0.13	6.17	0.61
353	5.00	4.11	1241.0	0.2	1.56	0.12	1.976	0.09	1.11	0.06	0.79	0.06	4.06	0.11

Table S7: Results of Continuous Fractional Component Monte Carlo (CFCMC) simulations to compute solubilities of H_2 and activities of water in aqueous $\text{NaB}(\text{OH})_4$ solutions using the DFF/ $\text{B}(\text{OH})_4^-$ model developed in this work (see Table 1 of the main text), combined with the Na^+ model of Madrid-2019,⁶ the TIP4P/2005¹ H_2O force field, and the Marx³ H_2 force field. T is in units of K, m is in units of mol $\text{NaB}(\text{OH})_4/\text{kg}$ water, and C is in units of mol $\text{NaB}(\text{OH})_4/\text{L}$ solution. $\mu_{\text{ex,w}}$ and $\mu_{\text{ex,H}_2}$ are the excess chemical potentials of water and H_2 (ideal gas reference state), respectively, and are in units of $k_{\text{B}}T$. a_{w} is the activity of water (dimensionless) and is computed by multiplying the activity coefficient of water (γ_{w}) with the mole fraction of water (x_{w}). x_{H_2} is the solubility (mole fraction) of H_2 in units of 10^{-5} at a H_2 partial pressure of 1 bar. σ_x is the standard deviation of quantity x . Rahbari et al.¹² have computed a chemical potential of $-10.86 \pm 0.14 k_{\text{B}}T$, (ideal gas reference state) for the TIP4P/2005 water force field¹ at 323 K and 100 bar (Table S4 of Ref.¹²). This agrees with the excess chemical potential obtained at 323 K and 1 bar in this work ($-10.71 \pm 0.01 k_{\text{B}}T$) (ideal gas reference state) considering the differences in pressure.

T	m	C	$\mu_{\text{ex,w}}$	$\sigma_{\mu_{\text{ex,w}}}$	a_{w}	$\sigma_{a_{\text{w}}}$	$\mu_{\text{ex,H}_2}$	$\sigma_{\mu_{\text{ex,H}_2}}$	x_{H_2}	$\sigma_{x_{\text{H}_2}}$
298	0.00	0.00	-12.21	0.03	1.00	0.00	4.04	0.01	1.29	0.01
298	0.93	0.89	-12.21	0.01	0.97	0.04	4.26	0.02	1.05	0.02
298	2.96	2.69	-12.24	0.02	0.89	0.05	4.69	0.01	0.70	0.01
298	5.00	4.27	-12.34	0.03	0.76	0.04	5.07	0.03	0.49	0.01
323	0.00	0.00	-10.71	0.01	1.00	0.00	4.04	0.01	1.20	0.00
323	0.93	0.88	-10.72	0.01	0.96	0.02	4.21	0.01	1.03	0.01
323	2.96	2.65	-10.76	0.01	0.87	0.01	4.56	0.01	0.75	0.01
323	5.00	4.20	-10.83	0.01	0.76	0.02	4.90	0.01	0.55	0.01
353	0.00	0.00	-9.27	0.01	1.00	0.00	3.93	0.01	1.25	0.01
353	0.93	0.87	-9.28	0.01	0.96	0.01	4.06	0.01	1.11	0.01
353	2.96	2.59	-9.32	0.01	0.86	0.01	4.36	0.01	0.85	0.01
353	5.00	4.10	-9.40	0.02	0.75	0.01	4.63	0.01	0.67	0.01

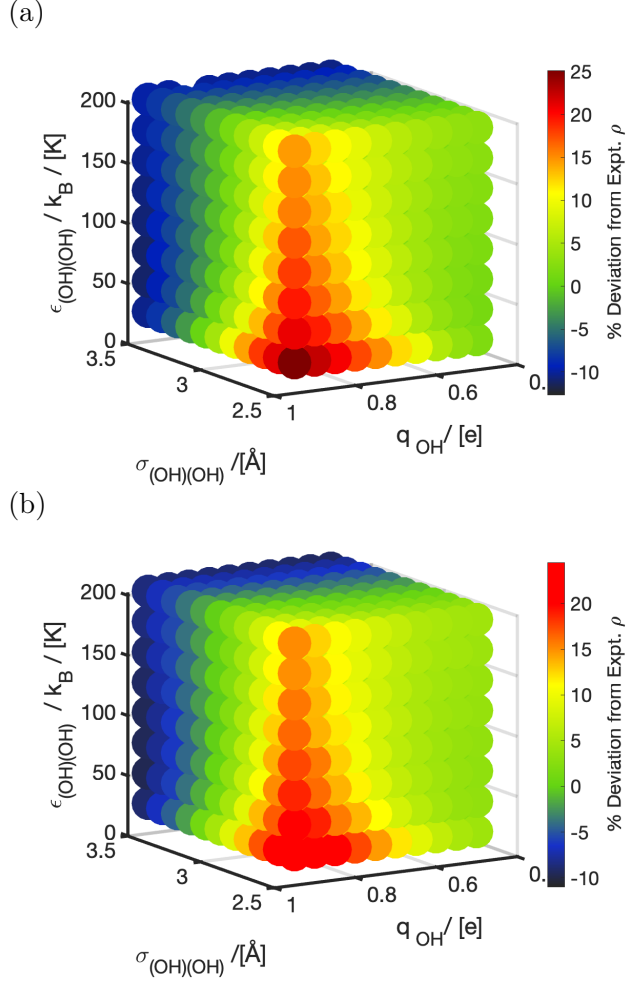


Figure S1: Percentage deviation of computed densities from experimental densities at a molality of 5 mole $\text{NaB}(\text{OH})_4/\text{kg}$ water at 298 K and 1 bar for ca. 900 different models of $\text{B}(\text{OH})_4^-$ with varying OH charges (q_{OH}), and Lennard-Jones parameters. $\sigma_{(\text{OH})(\text{OH})}$ is the LJ size parameter for OH-OH interactions. $\epsilon_{(\text{OH})(\text{OH})}$ is the LJ energy parameter for OH-OH interactions. For all other LJ interactions, the Lorentz-Berthelot mixing rules^{13,14} are used. The total charge of $\text{B}(\text{OH})_4^-$ equals $q_{\text{B}(\text{OH})_4} = q_{\text{B}} + 4 \times q_{\text{OH}}$, where q_{B} is the charge on the B atom. The charge q_{OH} is varied from $-0.95e$ to $-0.50e$ in steps of $0.05e$. The ab-initio simulations of Zhou et al.¹⁵ suggest a charge of ca. $0.55 e$ on the OH group of aqueous $\text{B}(\text{OH})_4^-$. A larger q_{OH} range is considered, as the charge distribution is viewed as an additional degree of freedom to obtain accurate densities and viscosities of aqueous $\text{NaB}(\text{OH})_4$ solutions. $\sigma_{(\text{OH})(\text{OH})}$ is varied from 2.5 \AA to 3.5 \AA in steps of 0.1 \AA and $\epsilon_{(\text{OH})(\text{OH})}/k_{\text{B}}$ is varied from ca. 25 K to 200 K in steps of 25 K . Both ranges are consistent with the $\text{B}(\text{OH})_4^-$ model developed by Zhou et al.¹⁵ and the atomistic Delft Force Field of OH^- (DFF/ OH^-) developed in our previous work.⁵ In (a), $q_{\text{B}(\text{OH})_4} = -0.85 [e]$ and the model is combined with the Madrid-2019 Na^+ model⁶ ($q_{\text{Na}} = +0.85 [e]$). In (b), $q_{\text{B}(\text{OH})_4} = -0.75 [e]$ and the model is combined with the Madrid-Transport Na^+ model⁴ ($q_{\text{Na}} = +0.75 [e]$). Based on these simulations, four different models are probed and listed in Table 1 of the main text to compute viscosities of aqueous $\text{NaB}(\text{OH})_4$ solutions.

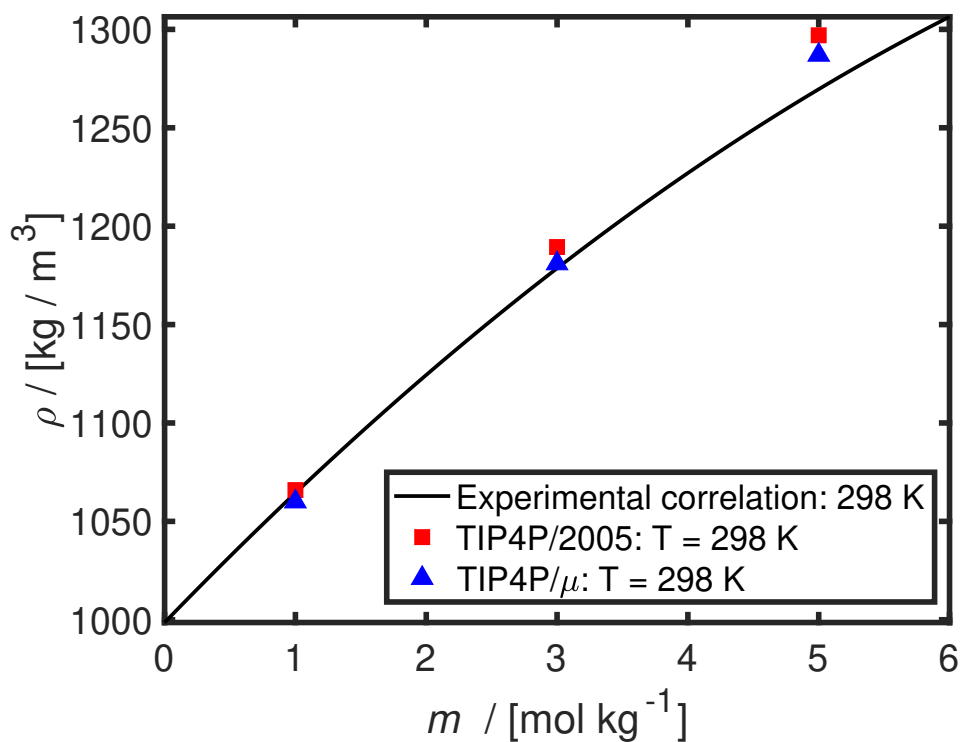


Figure S2: Computed densities of aqueous NaB(OH)_4 solutions using the DFF/ B(OH)_4^- force field developed in this work combined with the Madrid-2019 Na^+ force field⁶ at 298 K and 1 bar. Two different water force fields are considered to test the transferability of the DFF/ B(OH)_4^- force field, namely the TIP4P/2005¹ and the modified TIP4P/2005 (here denoted by TIP4P/ μ) of Rahbari et al.², which can accurately capture the saturated vapor pressure of water. The experimental correlation for the densities of aqueous NaB(OH)_4 at 298 K by Zhou et al.¹⁶ is shown as a solid line. It can be seen that for both water force fields, accurate densities of aqueous NaB(OH)_4 solutions can be obtained using the DFF/ B(OH)_4^- and Madrid-2019 Na^+ force fields.

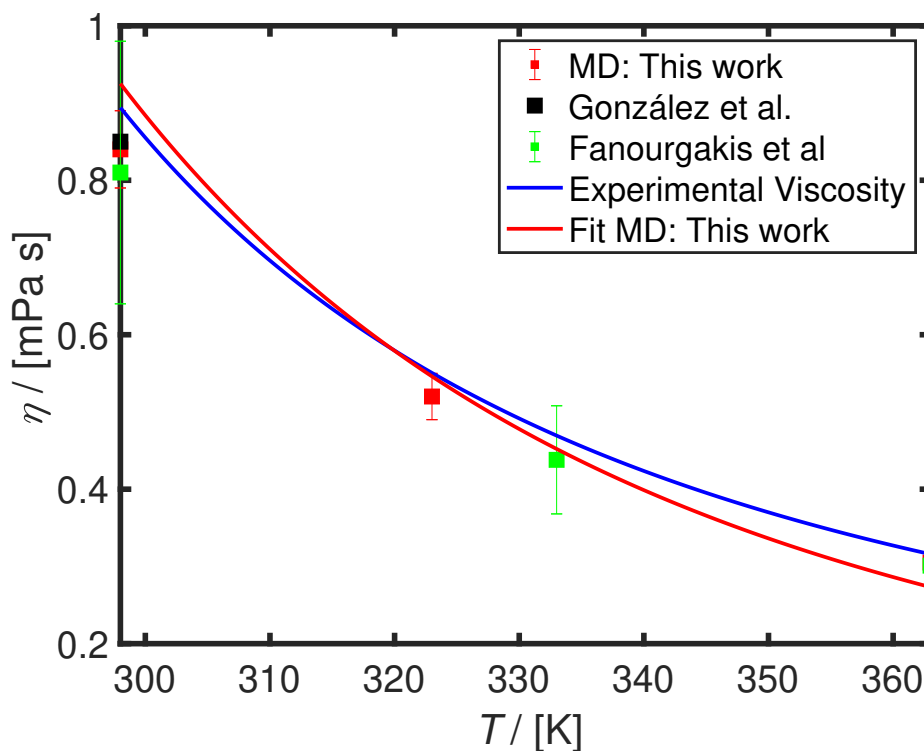


Figure S3: Computed viscosities of pure TIP4P/2005¹ using MD simulations for a temperature range of 298-363 K at 1 bar. The dynamic viscosities computed in this work are compared to other works of González and Abascal¹⁷ and Fanourgakis et al.¹⁸ for TIP4P/2005.¹ The results of this work are in quantitative agreement with these works. The blue solid line is based on the experimental correlation of Olsson et al.¹⁹ for pure water and the red solid line is viscosity correlation expressed in Eq. 9 of the main text at a NaB(OH)₄ molality of zero.

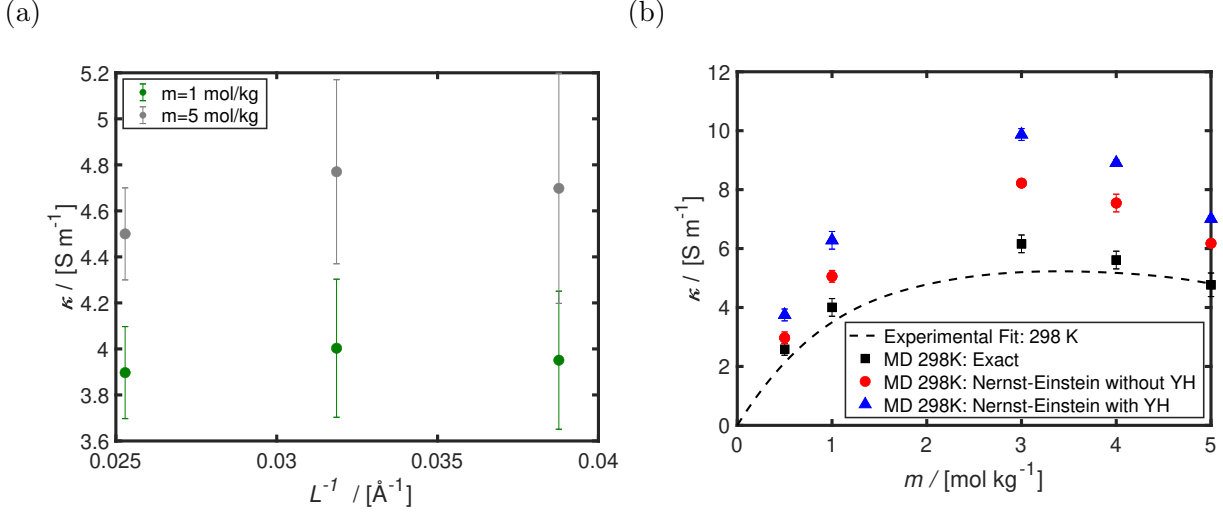


Figure S4: Computed electrical conductivities (κ) of aqueous NaB(OH)_4 as functions of (a) the reciprocal simulation cell box-size (L^{-1}) and (b) molality (m) in units of mol $\text{NaB(OH)}_4/\text{kg}$ water at 298 K and 1 bar. The electrical conductivities are computed from MD simulations using the DFF/ B(OH)_4^- model (see Table 1 of the main text) combined with the TIP4P/2005¹ water and Madrid-2019⁶ Na^+ force fields. In (a), the exact ionic conductivities (Eq. 1 of the main text) are computed for three different systems with 555, 1000, and 2000 water molecules for molalities (m) of 1 and 5 mol $\text{NaB(OH)}_4/\text{kg}$ water, respectively. For simulations with 1 mol $\text{NaB(OH)}_4/\text{kg}$ water, 10, 18 and 36 NaB(OH)_4 molecules are used for systems of 555, 1000, and 2000 water molecules, respectively. For simulations with 5 mol $\text{NaB(OH)}_4/\text{kg}$ water, 50, 90 and 180 NaB(OH)_4 molecules are used for systems of 555, 1000, and 2000 water molecules, respectively. For both concentrations, the finite-size effects are within the error bars (ca. 10%). In (b), the electrical conductivities are computed using the exact expression (Eq. 1 of the main text) and the Nernst-Einstein expression (Eq. 2 of the main text) and compared to the experimental conductivities of Zhou et al.¹⁶ (dashed lines). In (b), the Nernst-Einstein expression is evaluated using ion diffusivities, which are either corrected for finite-size effects using the Yeh-Hummer equation^{10,11} (Nernst-Einstein with YH) or uncorrected (Nernst-Einstein without YH). At the limit of $m \rightarrow 0$ the exact expression and NE expression without Yeh-hummer correction are equal by definition.

Literature Cited

- (1) Abascal, J. L.; Vega, C. A general purpose model for the condensed phases of water: TIP4P/2005. *Journal of Chemical Physics* **2005**, *123*, 234505.
- (2) Rahbari, A.; Garcia-Navarro, J. C.; Ramdin, M.; van den Broeke, L. J. P.; Moulτος, O. A.; Dubbeldam, D.; Vlugt, T. J. H. Effect of Water Content on Thermodynamic Properties of Compressed Hydrogen. *Journal of Chemical & Engineering Data* **2021**, *66*, 2071–2087.
- (3) Marx, D.; Nielaba, P. Path-integral Monte Carlo techniques for rotational motion in two dimensions: Quenched, annealed, and no-spin quantum-statistical averages. *Physical Review A* **1992**, *45*, 8968.
- (4) Blazquez, S.; Conde, M. M.; Vega, C. A. Scaled charges for ions: An improvement but not the final word for modeling electrolytes in water. *Journal of Chemical Physics* **2023**, *158*, 054505.
- (5) Habibi, P.; Rahbari, A.; Blazquez, S.; Vega, C.; Dey, P.; Vlugt, T. J. H.; Moulτος, O. A. A New Force Field for OH⁻ for Computing Thermodynamic and Transport Properties of H₂ and O₂ in Aqueous NaOH and KOH Solutions. *Journal of Physical Chemistry B* **2022**, *126*, 9376–9387.
- (6) Zeron, I. M.; Abascal, J. L. F.; Vega, C. A force field of Li⁺, Na⁺, K⁺, Mg²⁺, Ca⁺, Cl⁻, and SO₄²⁻ in aqueous solution based on the TIP4P/2005 water model and scaled charges for the ions. *Journal of Chemical Physics* **2019**, *151*, 104501.
- (7) Rahbari, A.; Hens, R.; Ramdin, M.; Moulτος, O. A.; Dubbeldam, D.; Vlugt, T. J. H. Recent advances in the Continuous Fractional Component Monte Carlo methodology. *Molecular Simulation* **2021**, *47*, 804–823.

- (8) Shi, W.; Maginn, E. J. Continuous Fractional Component Monte Carlo: an adaptive biasing method for open system atomistic simulations. *Journal of Chemical Theory and Computation* **2007**, *3*, 1451–1463.
- (9) Shi, W.; Maginn, E. J. Improvement in molecule exchange efficiency in Gibbs ensemble Monte Carlo: Development and implementation of the Continuous Fractional Component move. *Journal of Computational Chemistry* **2008**, *29*, 2520–2530.
- (10) Yeh, I.-C.; Hummer, G. System-size dependence of diffusion coefficients and viscosities from molecular dynamics simulations with periodic boundary conditions. *Journal of Physical Chemistry B* **2004**, *108*, 15873–15879.
- (11) Jamali, S. H.; Wolff, L.; Becker, T. M.; Bardow, A.; Vlugt, T. J. H.; Moulτος, O. A. Finite-size effects of binary mutual diffusion coefficients from molecular dynamics. *Journal of Chemical Theory and Computation* **2018**, *14*, 2667–2677.
- (12) Rahbari, A.; Brenkman, J.; Hens, R.; Ramdin, M.; Broeke, L. J. V. D.; Schoon, R.; Henkes, R.; Moulτος, O. A.; Vlugt, T. J. H. Solubility of water in hydrogen at high pressures: A Molecular Simulation study. *Journal of Chemical & Engineering Data* **2019**, *64*, 4103–4115.
- (13) Allen, M. P.; Tildesley, D. J. *Computer simulation of liquids*; Oxford University Press, 2017.
- (14) Frenkel, D.; Smit, B. *Understanding Molecular Simulation: from algorithms to applications*, 2nd ed.; Elsevier: San Diego, 2002.
- (15) Zhou, Y.; Higa, S.; Fang, C.; Fang, Y.; Zhang, W.; Yamaguchi, T. B(OH)_4^- hydration and association in sodium metaborate solutions by X-ray diffraction and empirical potential structure refinement. *Phys. Chem. Chem. Phys.* **2017**, *19*, 27878–27887.

- (16) Zhou, Y.; Fang, C.; Yang, Y.; Zhu, F. Volumetric and Transport Properties of Aqueous NaB(OH)_4 Solutions. *Chinese Journal of Chemical Engineering* **2013**, *21*, 1048–1056.
- (17) González, M. A.; Abascal, J. L. F. The shear viscosity of rigid water models. *The Journal of Chemical Physics* **2010**, *132*.
- (18) Fanourgakis, G. S.; Medina, J. S.; Prosimi, R. Determining the Bulk Viscosity of Rigid Water Models. *The Journal of Physical Chemistry A* **2012**, *116*, 2564–2570.
- (19) Olsson, J.; Jernqvist, Å.; Aly, G. Thermophysical properties of aqueous $\text{NaOH-H}_2\text{O}$ solutions at high concentrations. *International Journal of Thermophysics* **1997**, *18*, 779–793.